BNL--52248

DE90 014754

BNL-52248
UC-414
(High Energy Physics-
DOE/OSTI-4500-R75)

SNAKES AND SPIN ROTATORS

S.Y. Lee

June 18, 1990

Accelerator Development Department

Brookhaven National Laboratory
Associated Universities, Inc.
Upton, Long Island, New York 11973

Under Contract No. DE-AC02-76CH00016 with the

UNITED STATES DEPARTMENT OF ENERGY

Abstract

The generalized snake configuration offers advantages of either shorter total snake length and smaller orbit displacement in the compact configuration or the multi-functions in the split configuration. We found that the compact configuration can save about 10% of the total length of a snake. On the other hand, the split snake configuration can be used both as a snake and as a spin rotator for the helicity state. Using the orbit compensation dipoles, the split snake configuration can be located at any distance on both sides of the interaction point of a collider provided that there is no net dipole rotation between two halves of the snake. The generalized configuration is then applied to the partial snake excitation. Simple formula have been obtained to understand the behavior of the partial snake. Similar principle can also be applied to the spin rotators. We also estimate the possible snake imperfections due to various construction errors of the dipole magnets. Accuracy of field error of better than 10^{-4} will be significant.

Table of Contents

	Abstract	ii
1.	Introduction	1
2.	Modified Snake Configuration	2
	2.1 m>2 Case or the Compact Snake Configuration	3
	2.2 1<m<2 Case	4
	2.3 Bi-Sectional m=2 Snake	5
3.	Partial Snake	5
	3.1 Compact Partial Snake	5
	3.2 Split Partial Snake	6
4.	Snake Imperfections	7
5.	Conclusions	8
	References	8

List of Figures

Figure 1. The relation between ψ_x, ψ_y of the spin rotation angle for the H and V magnets are shown. The snake axis ϕ_s is also given as a function of ψ_y. 9

Figure 2. Schematic plot of the modified snake configuration. The length of the horizontal bending magnet mH is determined by the closed orbit geometry. 10

Figure 3. The spin rotation angles ψ_x and ψ_y are plotted for m=1.106, where the free space between the two halves of the snake is about 80 m. The spin direction ϕ_M in the middle of the snake is also shown. 11

Figure 4. Schematic plot of the split snake configuration, where the distance between the two halves of the snake does not depend on the geometry. In this scheme, the aperture requirement for the dipole magnet is reduced in comparison with that of Fig. 2 with m=1.106. 12

Figure 5. The aperture requirement and the relation between ψ_x and ψ_y are plotted for the 5% compact snake configuration with m=2.42. 13

List of Tables

Table 1. Length and Orbit Displacements for Snake Configurations 4

Table 2. Parameters for the Split Partial Snake 7

1. Introduction

Recently, K. Steffen[1] has discovered a families of snakes with the magnet sequence as

$$S = (-H,\ -V,\ 2H,\ 2V,\ -2H,\ -V,\ H)$$

where H and V are the horizontal and vertical bending magnets respectively. To satisfy the snake criteria, the sequence of magnets does not alter the particle orbit outside the snake and the spinor of the particle is transformed according to

$$e^{i\frac{\varphi}{2}\hat{n}_s\cdot\vec{\sigma}}\ .$$

where φ is the spin rotation angle. At $\varphi = \pi$, we have a 100% snake. The snake axis $\hat{n}_s = (\cos\varphi_s, \sin\varphi_s, 0)$ depends on the excitation of H and V magnets. The Steffen's snake configuration S can be summarized by the following equations

$$\cos^2\psi_y + \cos 2\psi_x \sin^2\psi_y = 0 \tag{1}$$

$$\sin\varphi_s = \sqrt{2}\ \cos\ \psi_x \tag{2}$$

where ψ_x and ψ_y are the spin rotation angle of H and V magnets. The relation between ψ_x and ψ_y in Eq. (1) ensures the snake condition of the magnet sequence. The snake axis can then be determined by Eq. (2). The spin rotation angle ψ_y is limited in the range between 45° and 135°. Figure 1 shows the ψ_x, ψ_y relationship of Eq. (1) and φ_s vs. ψ_y.

The integrated magnet strength is given by

$$\int Bd\ell = 1.746(6\psi_x + 4\psi_y)\ [\mathrm{Tm}] \tag{3}$$

Note that $\psi_y \in \pm[45^o, 135^o]$ and $\psi_x \in \pm[45^o, 90^o]$. The spin rotator axis φ_s depends on the excitation of ψ_x and ψ_y is also shown in Fig. 1. When $\varphi_s = 0$ or 180°, the snake axis is along the radial $\hat{x}$ axis. When $\varphi_s = 90^o$, the snake axis is in the longitudinal direction. Depending on the excitation of the horizontal and vertical dipoles, the integrated magnet strengths vary from 17 to 33 Tm.

The corresponding orbit displacements are given by

$$D_x = (\ell_x + \ell_y + 2\ell_g)\frac{\psi_x}{G\gamma} \tag{4}$$

$$D_y = (2\ell_x + \ell_y + 2\ell_g)\frac{\psi_x}{G\gamma} \tag{5}$$

Since the maximum orbit displacement is proportional to the lengths of the magnets, it is advantageous to use a shorter dipole magnet. Since the lengths of magnets are given by

$$\ell_x = 1.746\frac{\psi_x}{B[T]} \text{ [m]} \tag{6}$$

$$\ell_y = 1.746\frac{\psi_y}{B[T]} \text{ [m]} \tag{7}$$

Thus the length is inversely proportional to the constant magnetic field B in Tesla. At RHIC injection energy, we expect $B\gamma \simeq 50$ T with $B = 2$ Tesla and $\gamma \simeq 26.6$. The orbit displacement can vary from 4 cm to 24 cm depending on the choice of magnet excitation. Economical consideration would prefer snake configurations with a smaller orbit distortion and smaller integrated $\int Bd\ell$ of magnets.

The advantage of the Steffen snake configuration is that the snake axis $\vec{n}_s$ can be changed continuously by properly ψ_x and ψ_y excitation. However, this snake configuration suffers the rigid structure of magnet position. The minimum length requirement for the snake is given by

$$L = 6\ell_x + 4\ell_y + 6\ell_g + [\ell_x + 2\ell_g] \tag{8}$$

where ℓ_x, ℓ_y and ℓ_g are respectively lengths of the magnets H, V and the distance between adjacent magnets. The length of the snake configuration requires an extra space of $\ell_x + 2\ell_g$ in Eq. (3), which is a little bit too small to be useful and too large a space to be wasted.

In this paper, we shall address the modified magnet configuration for the snake. First it may be interesting to eliminate the wasted free space. Furthermore, it would be nice to divide the snake into two pieces, which can be fitted into two adjacent straight sections. To achieve these goals, we discuss the modified snake configurations and its applications in section 2. The idea is then applied to the partial snake in section 3. the imperfection in the snake construction is discussed in section 4. Conclusion is given in section 5.

2. Modified Snake Configuration

The essential feature of Steffen snake is the symmetric arrangement of vertical bending magnets and the anti-symmetric horizontal bending magnets. These features can be preserved by the following snake configuration

$$S_m = (-H,\ -V,\ mH,\ 2V,\ -mH,\ -V,\ H)$$

where m is a number determined by the geometry. When $m > 2$, the space between the magnets mH and $-mH$ can be minimized. When $1 < m < 2$, the snake can be

decomposed into two parts, where each part is a spin rotator while the combined result of these two parts works as a snake. The spin rotation angle φ and the snake axis angle φ_s are given by

$$\cos\frac{\varphi}{2} = \cos^2\psi_y + \cos m\psi_x \sin^2\psi_y \tag{9}$$

$$\cos\varphi_s = \frac{-\sin\frac{m\psi_x}{2}\cos\psi_y}{\sqrt{\cos^2\frac{m\psi_x}{2} + \sin^2\frac{m\psi_x}{2}\cos^2\psi_y}} \tag{10}$$

Note here that the $m\psi_x$ vs. ψ_y are the relevant variables in the equations to determine φ and φ_s. Thus φ_s is independent of m.

2.1 $m > 2$ Case or the Compact Snake Configuration

The total length of the snake can be minimized by a proper chosen m. Assuming that the distance between adjacent magnets is ℓ_g, the condition for zero orbit displacement outside the snake gives

$$(m-1)\left(\ell_y + \ell_g + \frac{1}{2}(m-1)\,\ell_x\right) = \ell_x + \ell_y + 2\ell_g\ , \tag{11}$$

where ℓ_x, ℓ_y are the lengths of magnets H and V respectively. The total length of the snake configuration is given by

$$L = 6\ell_x + 4\ell_y + 6\ell_g\ . \tag{12}$$

The snake property of the configuration is determined by Eqs. (9) and (10). The orbit displacements are given by

$$D_x = (\ell_x + \ell_y + 2\ell_g)\,\frac{\psi_x}{G\gamma} \tag{13}$$

$$D_y = (m\ell_x + \ell_y + 2\ell_g)\,\frac{\psi_y}{G\gamma} \tag{14}$$

Table 1 compares the snake configuration for $\varphi_s = 0^o, 45^o, 90^o, 135^o$ and 180^o snakes by assuming 2 Tesla magnetic field and $\ell_g = 0.15$ m. Note that the compact snake configuration, where m is obtained from Eq. (11), has a total length $1 \sim 2$ m less than that of the Steffen snake configuration ($m = 2$). The horizontal orbit displacement is reduced slightly, while the vertical orbit displacement remains the same in both cases [see Eqs. (9), (10) and (14)]. The total integrated $\int Bd\ell$ is also slightly smaller for the compact snake configuration.

Table 1. Length and Orbit Displacements for Snake Configurations $\ell_g = 0.15$ m.

m	ψ_x	ψ_y	ϕ_s	γD_x[m]	γD_y[m]	L[m]
2	90	45	180	2.06	1.63	13.54
2	60	54.74	135	1.13	1.58	10.94
2	45	90	90	1.03	2.67	11.49
2	60	125.26	45	1.82	4.92	15.24
2	90	135	0	3.27	6.70	19.03
2.334	77.12	45	180	1.62	1.63	11.48
2.289	52.42	54.74	135	0.99	1.58	9.49
2.209	40.74	90	90	0.91	2.67	10.37
2.191	54.77	125.26	45	1.62	4.92	13.86
2.215	81.26	135	0	2.84	6.70	17.09

2.2 $1 < m < 2$ Case

When the snake is separated into two parts at the symmetry point, the combined effect on the spin remains unchanged provided that there is no net spin precession in the region between two half–snakes. To accomplish this task, m can be determined from the geometry of Fig. 2, i.e.,

$$(m-1)\left(d+\ell_y+\frac{1}{2}(m-1)\,\ell_x+\ell_g\right)=\ell_x+\ell_y+2\ell_g\,. \tag{15}$$

With the vertical compensation dipoles, V' and $-V'$, the vertical orbit displacement in the central region will be zero.

The characteristics of the snake is governed by Eqs. (9) and (10). In the present scenario, the half–snake can be used either as a spin rotator or as a space saver, where the half–snake (V', $-V'$, $-H$, $-V$, mH, V) would occupy a straight section smaller than the full snake. To use the half–snake as a space saver, the accelerator lattice must possess adjacent straight sections. The horizontal orbital displacement is however slightly larger (see Eq. 13).

Using the half–snake as a spin rotator, besides its combined function as a snake, the helicity state of the spin particle can be achieved. For a spin up particle passing through the half snake, the spin components becomes

$$\begin{aligned} S_x &= -\sin m\psi_x \sin\psi_y \\ S_y &= \sin^2\frac{m\psi_x}{2}\sin 2\psi_y \\ S_z &= 0 \end{aligned}$$

Let ϕ_M be the angle of the spin relative to the radial $\hat{x}$ axis. We obtain then

$$\tan\phi_M = \frac{S_y}{S_x}$$

Figure 3 shows ϕ_M as a function of the ψ_y, the spin precession angle of the vertical bend magnet for $m = 1.106$. The available free space is 80 m in the central region. Such a scheme can save four spin rotators in the helicity experiment. The horizontal orbit displacement for $m = 1.1$ is about a factor of 2 larger than that of $m = 2$. The orbit displacement problem in the central region can always be compensated by local orbit bumps without net spin precession angle.

Due to the large orbit displacement in the horizontal direction for the long spatial separation between the two half–snakes, the present scheme may be impractical for RHIC. The scheme is however useful for the snake to be used in the adjacent straight section separated by a quadrupole. A practical design of the combined snake and spin rotator will be discussed in the next section.

2.3 Bi–Sectional $m = 2$ Snake

Since $m \simeq 1$ is needed to accommodate a large free space between the two halves of the snake, the orbit aperture becomes nearly a factor of 2 larger. The difficulty can be solved by the configuration of the snake shown in Fig. 4. Using the orbit compensation magnets $-H$ and H is the middle of the two halves, where $m = 2$ is restored. Similarly the $V', -V'$ magnet combination are used to correct the vertical orbit. In this scheme, the magnet excitation ψ_x, ψ_y and the snake axis φ_s are given by Fig. 1 discussed in the introduction. The spin direction in the free space is however rotated by an extra ψ_x angle. The free space 2d in Fig. 4 is adjustable provided that there is no residual dipole field in the straight section. The orbit displacement can be reduced by about a factor of 2 in comparison with that of Section 2.2.

3. Partial Snakes

3.1 Compact Partial Snake

The snake configuration discussed in section 2 can also be applied to the design of the partial snake. The total length of the partial snake can be minimized by a properly chosen m. Figure 5 (lower part) shows ψ_x vs. ψ_y for 5% snake. The total length of the 5% partial snake has a broad minimum of 2.556 m (with B = 2T) at $\psi_y = 13.25°$, while orbit displacements D_x, D_y can be optimized at $\psi_y \simeq 10.5°$. The length of the snake is

about 2.6 m when 2 Tesla magnets and 15 cm spacing between magnets are used. The corresponding 5% snake for $m = 2$ will be about 50 cm longer.

To optimize the orbit displacements, we choose the following parameters for 5% snake at the peak field of 2T with 15 cm space between magnets.

$$\begin{aligned} m &= 2.45484 \\ \psi_x &= 10.1359^\circ \quad (\ell_x = 0.1544 \text{ m}) \\ \psi_y &= 10.5^\circ \qquad (\ell_y = 0.1600 \text{ m}) \\ L_{tot} &= 2.6072 \text{ m} = 8.5537 \text{ ft} \\ \gamma D_x &= 6.06 \text{ cm} \\ \gamma D_y &= 8.58 \text{ cm} \end{aligned}$$

At 1.4T, 1.6T and 1.8T field strength, the snake reaches strengths of 2.47%, 3.22% and 4.06% respectively.

Such a partial snake construction can be used in AGS, where the snake is needed at $G\gamma > 7$. The corresponding orbit displacements are less than 2 cm. Since the orbit displacement is proportional to the magnet excitation strength, the orbital displacements in the 2.5% snake would be about 1.4 cm at $G\gamma = 7$. The snake can be adiabatically turned on and off by a single power supply. The quadratic dependence of the magnet strength can be seen easily from the power series expansion of Eq. (9), i.e.

$$\varphi \simeq 2m\psi_x\psi_y \tag{16}$$

Eq. (16) indicates that the snake strength φ depends on ψ_x and ψ_y in the bilinear form (see also the lower part of Fig. 5 for $\varphi = 9^\circ$). Similarly, the snake axis is given by

$$\varphi_s \simeq \frac{\pi}{2} + \frac{m\psi_x}{2} \tag{17}$$

Therefore all the partial snakes with small ψ_x and ψ_y to obtain minimum orbit displacement and total length has snake axis near the longitudinal direction. The type II snake, where $\varphi_s = 0$ or 180° requires large ψ_x. This characteristic feature appears in all kinds of snake configurations.

3.2 Split Partial Snake

For the low energy accelerator, a long free space is usually not easily accessible. However two straight sections separated by a quadrupole can be useful for the partial snake as

well. The length of the quadrupole determines the quantity m. Two halves of a snake can be optimized to occupy the available space. In Table 2 we list the snake configuration for $d = 0.45$ m and $B = 2$T, where the corresponding free space is 90 cm.

Table 2. Parameters for the Split Partial Snake.

% Snake	m	ℓ_x[m]	ℓ_y[m]	ℓ'_y[m]	γD_x(cm)	γD_y(cm)	$L_{1/2}$[m]
5	1.7903	0.2021	0.1676	0.3053	8.65	8.88	2.250
10	1.8585	0.2894	0.2286	0.4244	15.12	15.57	2.883

The ℓ_x, ℓ_y, ℓ'_y are the lengths of magnets H, V and V' shown in Fig. 2 respectively. D_x and D_y are the maximum the orbit displacements in the horizontal and vertical planes. $L_{1/2}$ is the total length of the half-snake including the vertical orbit correctors V' and $-V'$. Since the orbit displacements vary inversely with respective to the energy and vary proportional to the magnet excitation strength, the orbit displacement can be maintained to be less than 1 cm in the realistic application.

4. Snake Imperfections

Since the snakes are composed of transverse magnets, there are two possible random errors: dipole excitation and dipole rotation. These two types of errors can give rise to error in the spin precession angle $\Delta\varphi$ and in the snake axis $\Delta\varphi_s$ of the order

$$\Delta\varphi_s \sim \Delta\varphi \sim \sqrt{(m\Delta\psi_x)^2 + (\Delta\psi_y)^2 + (\Delta\theta_R)^2}$$

where $\Delta\psi_x$, $\Delta\psi_y$ and $\Delta\theta_R$ are rms errors in the H, V magnets and dipole rotation respectively. These errors should be in the order of 10^{-3}, which give rise to the same order of magnitude of errors in $\Delta\varphi_s$ and $\Delta\varphi$. The tolerance of the error discussed in ref. 2 is much larger. Besides the random error, the dependent of φ and φ_s on the systematic error can be obtained by

$$\Delta\varphi = \left[\left(\frac{\partial\varphi}{\partial\psi_x}\right)^2 (\Delta\psi_x)^2 + \left(\frac{\partial\varphi}{\partial\psi_y}\right)^2 (\Delta\psi_y)^2 \right]^{1/2}$$

$$\Delta\varphi_s = \left[\left(\frac{\partial\varphi_s}{\partial\psi_x}\right)^2 (\Delta\psi_x)^2 + \left(\frac{\partial\varphi_s}{\partial\psi_y}\right)^2 (\Delta\psi_y)^2 \right]^{1/2}$$

Figure 1 shows clearly that the snake axis φ_s is much more sensitive to ψ_y for the type II snakes, where $\varphi = 0$ or π.

We obtain from Eqs. (9,10) that

$$\Delta\varphi \simeq \pm 2\left[\cot\frac{m\psi_x}{2}\Delta(m\psi_x) \pm 2\cot\psi_y\ \Delta\psi_y\right]$$

$$\Delta\varphi_s = \left(\pm\Delta\psi_y - \frac{\sqrt{2}}{2}\cos\frac{m\varphi_x}{2}\cos\psi_y\ \Delta(m\psi_x)\right) / \sin\varphi_s$$

Due to $\sin\varphi_s$ in the denominator, the type II snake is much harder to maintain its accuracy in the snake axis. It is preferable to tune the snake away from the $\varphi_s = 0$ or π.

Finally for the split configuration discussed in Section 2.3, the accuracy in the orbit compensation magnets $-H$ and H is also important. The snake axis will deviate from the horizontal plane by an angle equal to the net spin rotation angle of $-H$ and H magnets.

The antisymmetric insertion in the RHIC and SSC can also give rise to a net spin rotation for large amplitude particles. Using the RHIC lattice function, we expect a net spin rotation angle of 6×10^{-2} radian for the largest amplitude particle (35 mm from the center of the quadrupole) at the top energy. The effect decreases with increasing β^* value at the collision point. Since the large amplitude particle executes betatron motion, the snake axis will oscillate around the desired value with betatron frequency. Small amplitude oscillation of the spin tune around 1/2 will be an interesting problem to be studied. To minimize the effect, we can decrease the betatron amplitude at the high β quadrupoles. However the luminosity will be correspondingly smaller.

5. Conclusions

The generalized snake configuration has been found to be useful in realistic applications for either compact or split geometries. The basic properties of these snakes configurations has been studied. We found that the split snake can be used as a snake as well as the spin rotator for the helicity state. The generalized snake structure can be applied to a partial snake, which can be optimized to minimize orbit displacements and the total length of the magnets. Such an optimization is usually needed for the small accelerator, where the length of the straight section is small. Error analysis of the snake is also discussed.

References

1. K. Steffen, Particle Accelerators, 24, 45 (1989).
2. S.Y. Lee and E.D. Courant, Phys. Rev. **D41**, 292 (1990).

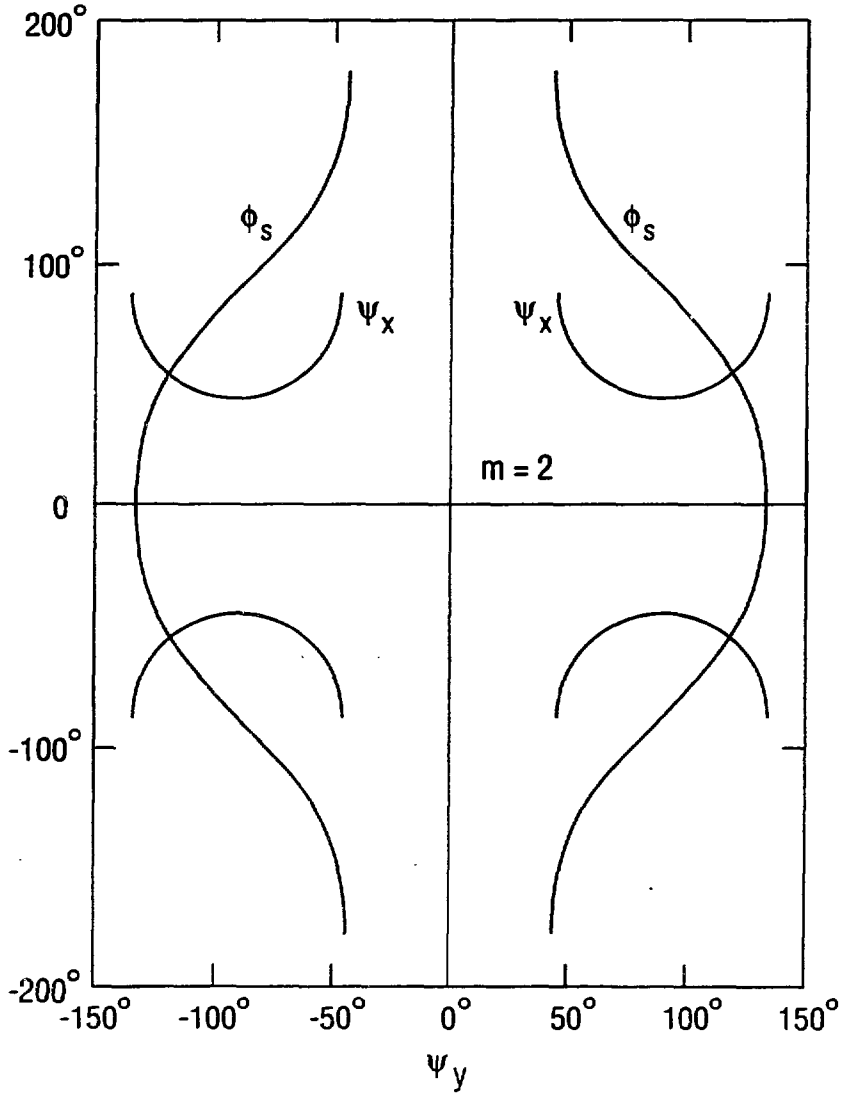
200°
100°
0
-100°
-200°
-150°
-100°
-50°
0°
50°
100°
150°
ψ_y
ϕ_s
ψ_x
ϕ_s
ψ_x
m = 2

Figure 1.

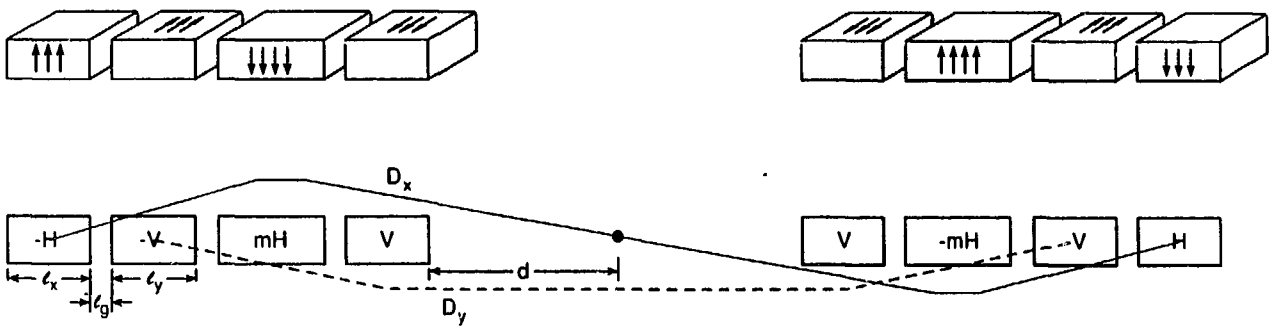

$$(m-1)\left(d+\tfrac{1}{2}(m-1)\ell_x+\ell_y+\ell_g\right)=\ell_x+\ell_y+2\ell_g$$

Figure 2.

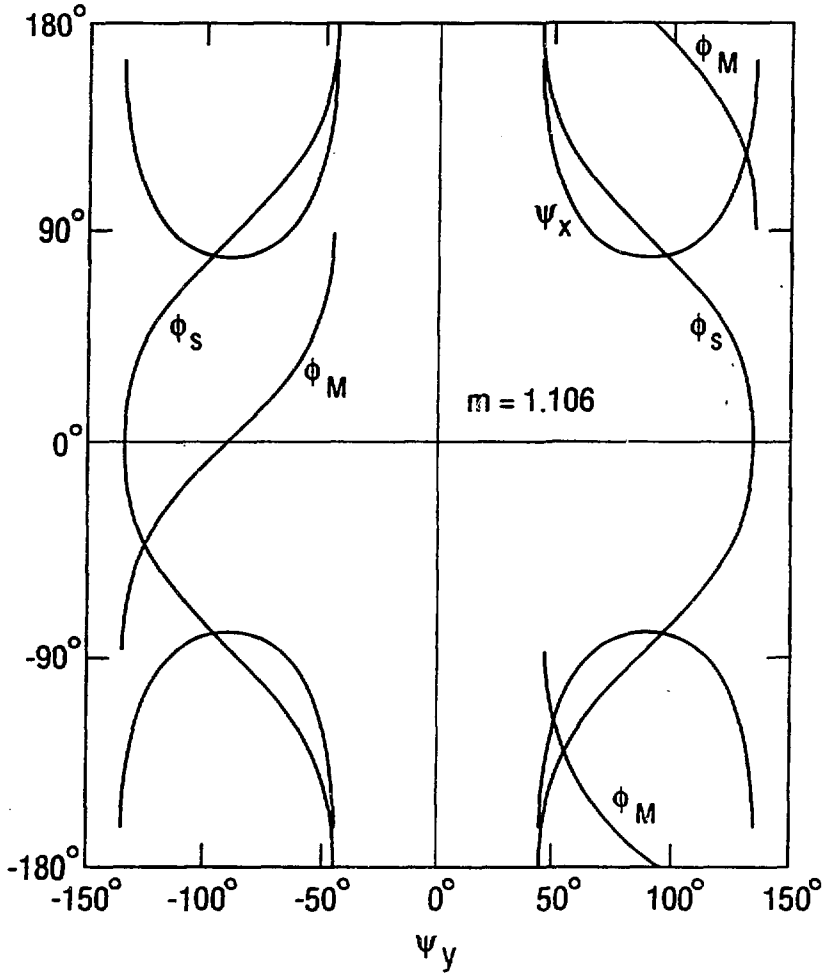
180°
90°
0°
-90°
-180°
-150°
-100°
-50°
0°
50°
100°
150°
Ψ_y
ϕ_S
ϕ_M
Ψ_x
ϕ_S
ϕ_M
m = 1.106
ϕ_M

Figure 3.

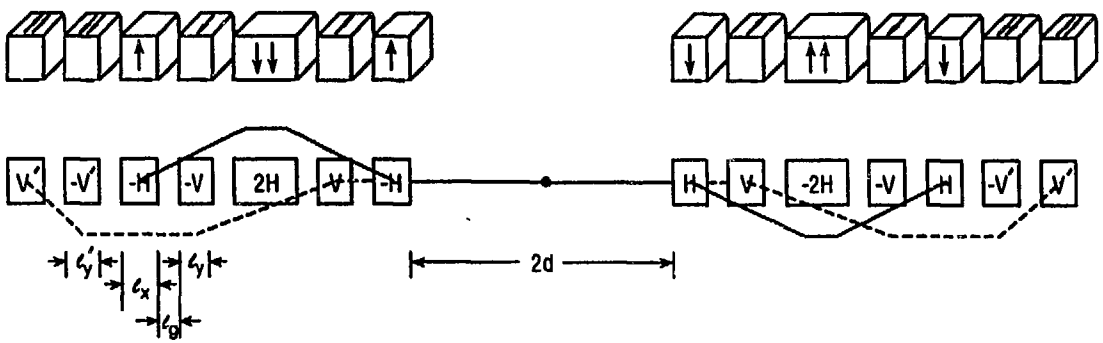

$$\ell_y(2\ell_x+\ell_y+2\ell_g)=(\ell_y'+\ell_g)\ell_y'$$

Figure 4.

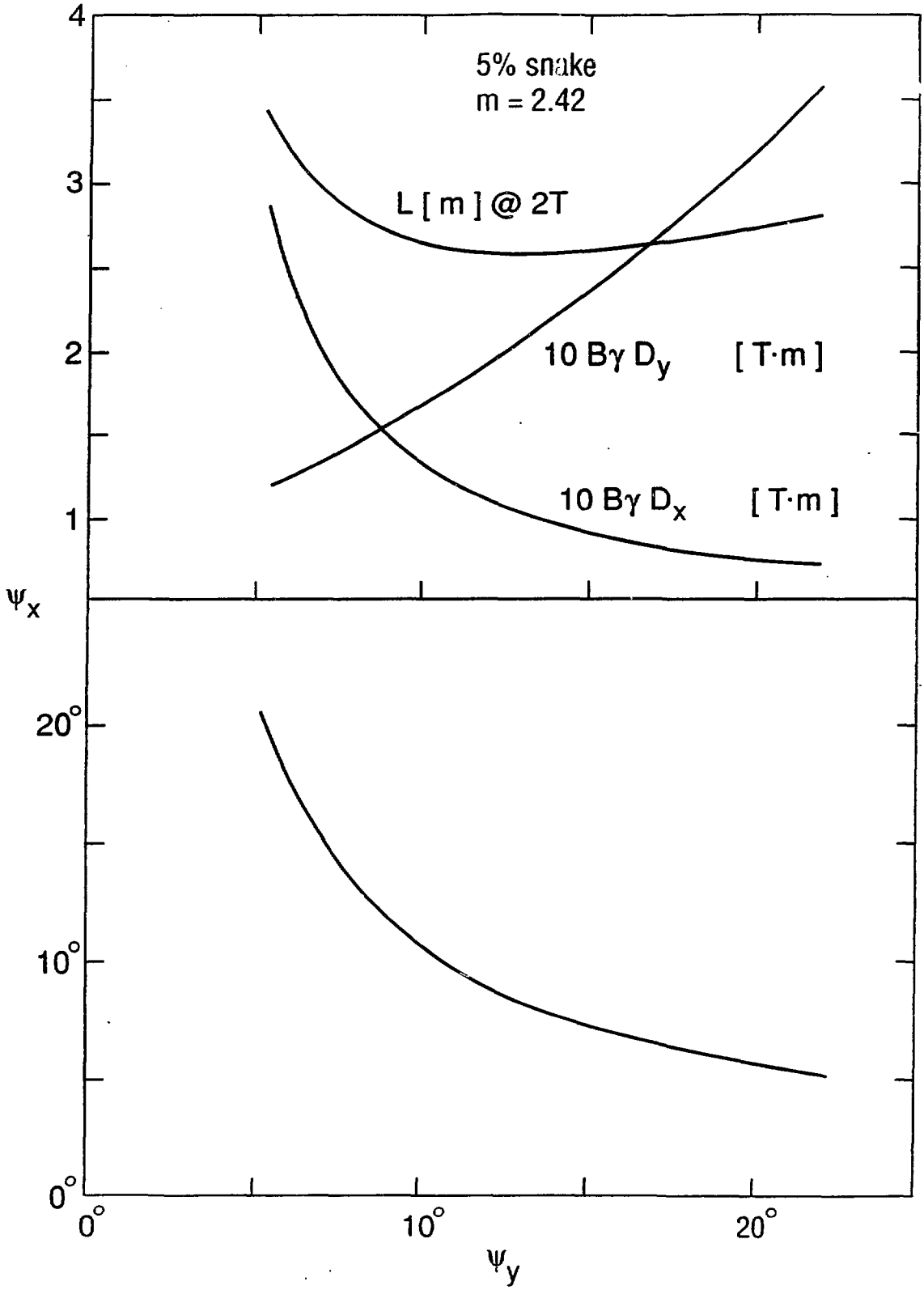
5% snake
m = 2.42
L [m] @ 2T
10 Bγ D_y [T·m]
10 Bγ D_x [T·m]
ψ_x
ψ_y
4
3
2
1
20°
10°
0°
0°
10°
20°

Figure 5.